Microrheology of polyethylene oxide using diffusing wave spectroscopy and single scattering

Bivash R. Dasgupta,[1] Shang-You Tee,[1] John C. Crocker,[2] B. J. Frisken,[3] and D. A. Weitz[1]
[1]*Department of Physics and DEAS, Harvard University, Cambridge, Massachusetts 02138*
[2]*Department of Chemical Engineering, University of Pennsylvania, Philadelphia, Pennsylvania 19104*
[3]*Department of Physics, Simon Fraser University, Burnaby, British Columbia, Canada V5A 1S6*
(Received 27 November 2001; published 20 May 2002)

Experiments investigating the local viscoelastic properties of a simple uncross-linked flexible polymer are performed on polyethylene oxide solutions in the semidilute regime using polystyrene beads of varying sizes and surface chemistry as probes. We measure the thermal motions of the beads to obtain the elastic and viscous moduli of our sample. Two different dynamic light scattering techniques, diffusing wave spectroscopy and quasielastic light scattering (QELS), are used to determine the dynamics of the probe particles. Diffusing wave spectroscopy probes the short time dynamics of the scatterers while QELS or single scattering measures the dynamics at larger times. This results in a larger frequency overlap of the data obtained from the microrheological techniques with the data obtained from the conventional bulk measurements. The moduli are estimated using a modified algebraic form of the generalized Stokes-Einstein equation. Comparison of microrheology with bulk measurements shows excellent similarity confirming the applicability of this method for simple, uncross-linked polymeric systems.

DOI: 10.1103/PhysRevE.65.051505 PACS number(s): 83.85.Ei, 83.85.Cg, 83.10.Pp

I. INTRODUCTION

Soft materials such as gels and polymer solutions can have complex structures with characteristic length and time scales. The response of any material to shear strain is an important way of characterizing and understanding its structure. On application of a shear strain, solids store energy and are elastic, while fluids dissipate energy and are viscous. Some materials exhibit both these properties and are *viscoelastic* in nature. These complex fluids can be characterized by the stress relaxation modulus $G_r(t)$, which describes the magnitudes and time scales of the relaxation of the stress in the bulk material to a fixed strain after a step shear [1]. The Fourier transform of the stress relaxation modulus is the frequency-dependent complex shear modulus $G^*(\omega)$. The real part of the complex modulus $G'(\omega)$ measures the in phase response of the medium to an oscillatory strain and thus gives a measure of the elasticity of the material. The out of phase response is given by the imaginary part $G''(\omega)$, which is related to the viscosity of the material. The elastic and loss moduli are dependent on each other and are related by the Kramers-Kronig relations [2]. The measurement of bulk viscoelastic properties can be accomplished by means of a mechanical rheometer where, for example, the stress response of the material to an applied oscillatory strain provides a measure of the storage and loss moduli. Over the past few years, other complementary techniques have been developed, which have permitted the measurement of the local viscoelastic behavior of soft materials [3–8]. Several of these entail the use of localized probes of the viscoelasticity and have come to be called *microrheology*. Microrheological techniques typically require a few hundred microliters of sample as compared to several milliliters of sample as typically required for conventional bulk measurements; hence they are extremely useful for the measurement of the viscoelastic properties of costly or rare biological materials or industrial polymers. Microrheological techniques are also intrinsically noncontact, equilibrium methods for measuring the rheological properties of complex fluids. However, despite the great promise of microrheological techniques, the method has still not been extensively tested in diverse systems to ascertain that it measures the same response of the system as does the more traditional, mechanical rheological measurements.

The goal of this paper is to carefully test the validity of the microrheological measurements of polymer solutions, where a low concentration of probe particles are added to the solution and the thermal motion of these particles is used to determine the viscoelastic response of the host polymer solution. We focus here exclusively on uncross-linked polymer solutions, as examples of the simplest systems that can provide a critical test of microrheology while still exhibiting interesting behavior.

Two different dynamic light scattering (DLS) techniques, traditional quasielastic light scattering (QELS) [9] and diffusing wave spectroscopy (DWS) [10–12], are used to measure the dynamics of the tracer particles suspended in the polymer solution. Quasielastic light scattering measurements, which are made in the single scattering limit, determine the dynamics of the particle at larger length scales and longer time scales than DWS, where measurements are made in samples where multiple scattering dominates. Combining the two techniques allows us to probe frequencies ranging from 10^{-1} to 10^{5} rad/s. The extended frequency range is a key advantage of microrheology; traditional measurements using a rheometer can be extended over a limited range, determined primarily by the inertia of the measuring tool, and extending the frequency range is only possible in a limited number of cases though the use of time-temperature superposition [1,13]. We use two different molecular weights of polyethylene oxide (PEO) at different concentrations above the overlap concentration c^* to obtain samples with different viscoelastic properties. Polystyrene beads of different sizes and chemistry are used as our probe particles to test

the effect of particle size and surface properties on the measurement. We introduce a modified form of the method of analysis first proposed by Mason [14] to obtain the elastic and viscous moduli from the light scattering data. In our method, a different algebraic form of the generalized Stokes-Einstein equation is used to calculate the frequency dependent moduli. This eliminates the need for numerical transforms of the experimental data and does not require an arbitrary functional form to fit the data and calculate the moduli [4,15]. Our modifications include a more accurate algebraic representation of the generalized Stokes-Einstein equation. To check the microrheology measurements, we compare the results from our light scattering measurements with those obtained using a strain-controlled rheometer.

II. THEORY AND METHOD OF ANALYSIS

Dynamic light scattering experiments can measure the time evolution of the mean square displacement $\langle \Delta r^2(\tau)\rangle$ of the probe particles suspended in a polymer solution. The mean square displacement (MSD) of the beads reflects the response of the material to the stress applied to it by the thermal motion of the beads. We can understand the relationship between the MSD and the response of the material quite clearly for two limiting cases: a purely viscous fluid and a completely elastic medium. If the material is purely viscous, the probe particles will diffuse through it and the MSD will increase linearly with time $\langle \Delta r^2(\tau)\rangle = 6D\tau$. By determining the diffusion coefficient D, one can calculate the viscosity of the material $\eta = k_B T/6\pi Da$ where a is the radius of beads. By contrast, the motion of the probe particles in an elastic medium will be constrained and the MSD will reach an average plateau value $\langle \Delta r_p^2\rangle$ that is set by the elastic modulus of the material. By equating the thermal energy $k_B T$ of each bead with its elastic energy $\frac{1}{2}\kappa\langle \Delta r_p^2\rangle$ where κ is the effective spring constant that characterizes the elasticity of the surrounding medium, an expression for the spring constant $\kappa \sim k_B T/\langle \Delta r_p^2\rangle$ can be obtained. The elastic modulus $G'(\omega)$ is related to the spring constant by a factor of length, which is the bead radius, a. Using such an energy balance argument, we can obtain a relation between the elastic modulus and the MSD, $G'(\omega) \sim k_B T/\langle \Delta r_p^2\rangle a$. This simplified picture highlights the essential physics behind this technique.

In general, the full frequency dependence of the viscoelastic moduli is obtained from the MSD by using the generalized Stokes-Einstein equation [4,15],

$$\tilde{G}(s) = \frac{k_B T}{\pi a s \langle \Delta \tilde{r}^2(s)\rangle}, \tag{1}$$

where $\langle \Delta \tilde{r}^2(s)\rangle$ is the Laplace transform of the mean square displacement $\langle \Delta r^2(\tau)\rangle$ and $\tilde{G}(s)$ is the viscoelastic spectrum as a function of the Laplace frequency s. Using Eq. (1), we can determine the macroscopic viscoelasticity of the material from the local response assuming that the bulk stress relaxation has the same behavior as the local relaxations that affect the bead dynamics.

In earlier implementations of this data analysis [4,15], the MSD in real space is transformed into Laplace space to obtain $\tilde{G}(s)$ using Eq. (1). An arbitrary functional form is fit to $\tilde{G}(s)$ and the modulus is expressed as a complex function in Fourier space by substituting $s \rightarrow i\omega$ in the functional form used for fitting the experimental data. The modulus in Laplace frequency space, $\tilde{G}(s)$, is transformed to Fourier frequency space to allow comparison with bulk mechanical measurements where the elastic and the viscous moduli are expressed in the Fourier frequency domain. It is important to note, however, that no additional information about the viscoelasticity of the material is gained by using instead $G^*(\omega)$ instead of $\tilde{G}(s)$ because both represent $G_r(t)$ after either a Fourier or a Laplace transformation. The method is essentially an analytic continuation of the real data into the complex plane. Limitations of this scheme include truncation errors introduced by numerical transformation of data over a limited range, and the requirement of an appropriate functional form to fit to $\tilde{G}(s)$.

Recently, Mason *et al.* [8,14] developed an alternative method of obtaining the viscoelastic moduli from the dynamics of the probe particles. In this method, the complex shear modulus is estimated *algebraically* by using a local power law to describe the mean square displacement of the beads in the complex fluid. This method of analysis eschews the use of any numerical transforms or arbitrary functional forms. The power law behavior is determined from the logarithmic time derivative of the MSD. For a particle in a purely viscous medium undergoing diffusive motion, the slope of the logarithmic time derivative of the MSD will be one, whereas for a probe in an elastic environment, where its motion is completely arrested, the slope of the MSD will be zero. Therefore, for a complex viscoelastic fluid, the logarithmic time derivative of the MSD will lie between zero and one. In this method, the Fourier space representation of the generalized Stokes-Einstein equation given in Eq. (1) is used [14],

$$G^*(\omega) = \frac{k_B T}{\pi a i\omega \Im\{\langle \Delta r^2(\tau)\rangle\}} \tag{2}$$

where $\Im\{\langle \Delta r^2(\tau)\rangle\}$ is the Fourier transform of the MSD. Assuming a local power law form for $\langle \Delta r^2(\tau)\rangle$ leads to the elastic $G'(\omega)$ and the loss $G''(\omega)$ moduli, which are given by [14]

$$G'(\omega) = G(\omega)\cos[\pi\alpha(\omega)/2], \tag{3}$$

$$G''(\omega) = G(\omega)\sin[\pi\alpha(\omega)/2],$$

where

$$G(\omega) = \frac{k_B T}{\pi a \langle \Delta r^2(1/\omega)\rangle \Gamma[1+\alpha(\omega)]}. \tag{4}$$

In Eq. (4), $\langle \Delta r^2(1/\omega)\rangle$ is the magnitude of $\langle \Delta r^2(\tau)\rangle$ evaluated at $\tau = 1/\omega$. The local power law $\alpha(\omega)$ is given by $|[\partial \ln\langle \Delta r^2(\tau)\rangle/\partial \ln \tau]|_{\tau=1/\omega}$ and Γ denotes the gamma function. The gamma function is a result of the Fourier transform

of the power law behavior of the mean square displacement. These functions are chosen to satisfy the Kramers-Kronig relations.

While this scheme is convenient to use, Eqs. (3) and (4) fail to give an accurate estimate for the moduli when the MSD is highly curved and its slope is changing rapidly. This region is one of particular interest, since it occurs where the value of the two moduli are equal, reflecting an important relaxation time of the sample. In addition, the algebraic estimate of the smaller of the two moduli can be in error by a factor of almost two at the extremes of the frequency range. To redress these shortcomings we have empirically modified Eqs. (3) and (4) by including second-order logarithmic time derivatives of the MSD [16]. This modification helps account for the curvature, gives a better estimate of the moduli in the curved regions of the data, while also improving the results for the smaller modulus. This scheme works best with at least 7 to 10 data points for each decade; however, it is sensitive to long wavelength ripples in the data. The modified equations that are used for extracting the moduli are

$$G'(\omega)=G(\omega)\{1/[1+\beta'(\omega)]\} \times\cos\left[\frac{\pi\alpha'(\omega)}{2}-\beta'(\omega)\alpha'(\omega)\left(\frac{\pi}{2}-1\right)\right], \quad (5)$$

$$G''(\omega)=G(\omega)\{1/[1+\beta'(\omega)]\} \times\sin\left[\frac{\pi\alpha'(\omega)}{2}-\beta'(\omega)[1-\alpha'(\omega)]\left(\frac{\pi}{2}-1\right)\right],$$

where

$$G(\omega)=\frac{k_BT}{\pi a\langle\Delta r^2(1/\omega)\rangle\Gamma[1+\alpha(\omega)][1+\beta(\omega)/2]}. \quad (6)$$

The second-order logarithmic time derivative of the MSD data is denoted by $\beta(\omega)$, while $\alpha'(\omega)$ and $\beta'(\omega)$ denote the local first- and second- order logarithmic derivatives of $G(\omega)$, respectively. A second-order polynomial fit using a sliding Gaussian window is used to numerically calculate the local first- and second-order logarithmic derivatives and to smoothen the data. We use Eq. (6) to obtain $G(\omega)$ from the MSD data using the above procedure. We then use the remaining two equations given in Eq. (5) and repeat the local power law fitting on $G(\omega)$ to obtain the elastic and loss moduli. The expressions in Eqs. (5) and (6) are based on the approximate algebraic expression for the storage and loss moduli given in Eqs. (3) and (4) and have been derived empirically.

In order to check the accuracy of the expressions in Eqs. (5) and (6), we test them with simulated data of the form

$$G^*(\omega)=(i\omega)^a+(i\omega)^b, \quad (7)$$

with each of the exponents varying from 0 to 1 in steps of 0.05. The frequency range chosen for our test ranged from 10^{-5} rad/s to 10^5 rad/s. This particular form of the modulus is chosen because it broadly captures the nature of the experimental data. Slopes of one and zero correspond to viscous fluids and elastic materials, respectively. The sum of two exponents enables us to simulate the crossover or the knee region between the two extreme limits. Materials that are neither strongly elastic nor predominantly viscous will lie in this knee region of the complex modulus. We compare the approximate results obtained from Eq. (5) with the exact values obtained from Eq. (7) for both the real and the imaginary parts.

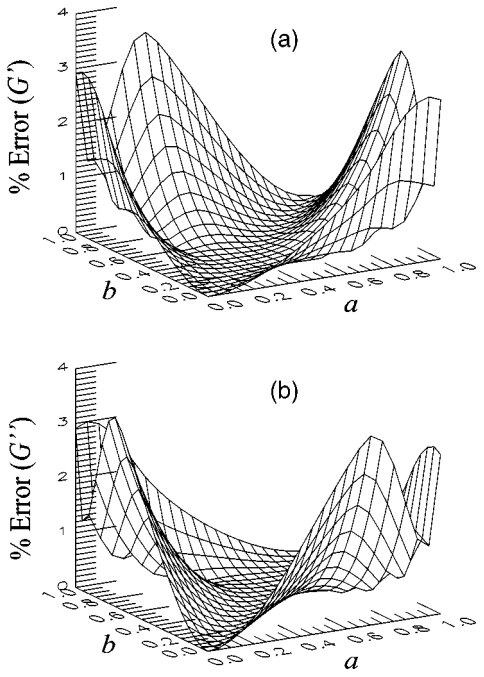

FIG. 1. Surface plot of the maximum error over the entire frequency range in the estimation of the (a) elastic $[G'(\omega)]$ and (b) viscous $[G''(\omega)]$ moduli obtained from data simulated using Eq. (7). The *x* and *y* axes denote the exponents used in Eq. (7) and the *z* axis denotes the difference between the values calculated using Eqs. (5) and (7). The accuracy of the estimated elastic and loss moduli lies within 4% of the exact value over the entire parameter space. The error is normalized by the larger of the two moduli.

Figure 1 is a three-dimensional plot of the maximum error over the entire frequency range in the estimation of both the elastic [Fig. 1(a)] and the viscous [Fig. 1(b)] moduli for each set of exponents. The *x* and *y* axes in the graph denote the exponents and of the simulated function given in Eq. (7). The error at each frequency is calculated by taking the difference between the approximate and the exact values of the moduli, and is normalized by the larger of the two moduli at that frequency. The maximum error in each modulus is less than 4% over the whole frequency range for the family of curves represented by Eq. (7). The maximum curvature for the set of curves obtained from the simulated function is 0.19, indicating that our method of analysis will result in reliable values of the moduli for any curve with a smaller radius of curvature. When one component of the modulus is much weaker than the dominant component, the relative errors can be larger than the error quoted above; however, these data are generally less reliable and are typically neglected. This method is sensitive to rapid fluctuations of the MSD data which occur at the two frequency extremes and which affect

the last few measurements at either end of the frequency range. Since our analysis uses the local power law fitting twice to obtain the moduli in frequency space from the MSD data, the error in the estimation of the moduli is less than 6% of the large modulus. For comparison, we also calculated the moduli using Eqs. (3) and (4) for data simulated using Eq. (7). In this case, the maximum error for each modulus over the entire simulated space was approximately 40% of the bigger modulus. This highlights the improved estimation of these modified algebraic forms.

We employ two different DLS techniques, QELS and DWS, to measure the bead dynamics and to obtain the evolution of the MSD with time. Diffusing wave spectroscopy extends the application of QELS to samples dominated by multiple scattering, using a *diffusive* approximation to describe the propagation of light through the sample. Similar to QELS, the decay of the autocorrelation function of the multiply scattered light, which is measured with DWS results from the change in the phase of the scattered light by $\sim\pi$. However, here the change in phase of the scattered light is caused by a change in the total path length of the light through the sample by one wavelength. Because the light is scattered many times in each path, any individual scatterer need move only a small fraction of the total wavelength of the incident light; nevertheless, the aggregate change of the total path length is one wavelength. As a result, this technique is sensitive to motion at shorter length scales and hence faster time scales than conventional light scattering. In DWS, all scattering-vector information is lost; as a result, only two experimental geometries, transmission and backscattering are used [11]. The field autocorrelation function at a delay time τ is [11]

$$g_1(\tau)\propto\int_0^\infty P(s)\exp\left[-k_o^2\langle\Delta r^2(\tau)\rangle\frac{s}{3l^*}\right]ds, \tag{8}$$

where $P(s)$ is the probability of light traveling a path of length s, and is determined by solving the diffusion equation for the propagation of light for the relevant geometry and with the correct boundary conditions, $k_o=2\pi/\lambda$ is the wave vector of the incident light and λ is the wavelength of light in the medium. The transport mean free path of the light, l^*, is a characteristic of the sample itself and reflects the amount of scattering; it is the length light must travel before its direction is randomized. The transport mean free paths for the samples used in these experiments are roughly four to ten times smaller than the cell thickness depending on the bead size used, ensuring strong multiple scattering. The expression for the field autocorrelation function given in Eq. (8) represents an incoherent sum over all light paths weighted by the probability of the light having a path of that length. A path of length s corresponds to a random walk of s/l^* steps and each step contributes a decay of $\exp[-k_o^2\langle\Delta r^2(\tau)\rangle/3]$ to the decay of the correlation function of that path.

Quasielastic light scattering measurements are performed on samples with weaker scattering ensuring only a single scattering event; they extend the time scales probed, enabling us to investigate a wider range of frequencies. In QELS, the individual scatterers must move a length scale set by the inverse of the scattering vector q in order to cause a change in the path length of the scattered light by one wavelength. Since the scatterers must move larger distances, the characteristic decay times are larger than those obtained in DWS. In this case, the field autocorrelation function is given by [9]

$$g_1(\tau)=\exp[-q^2\langle\Delta r^2(\tau)\rangle/6], \tag{9}$$

where $q=(4n\pi/\lambda)\sin(\theta/2)$, θ is the scattering angle, and n is the refractive index of the medium.

For both light scattering techniques, the time averaged intensity correlation function $g_2(\tau)$ is measured and the time averaged field correlation function $g_1(\tau)$ is obtained by using the Siegert relation [9]. The mean square displacement $\langle\Delta r^2(\tau)\rangle$ of the probe particles for the single scattering experiments is calculated from the field correlation functions using Eq. (9) above. For DWS experiments, the MSD is calculated by numerically inverting the field correlation functions and using the measured transport mean free path l^*.

III. EXPERIMENTAL DETAILS

We use PEO of two molecular weights, 200 kDa and 900 kDa, each at three different concentrations that range from 15 to 45 times greater than the overlap concentration, c^*; at these concentrations the solution begins to exhibit significant viscoelasticity due to the entanglement of the polymer coils. The overlap concentration marks the onset of the semidilute regime of a polymer solution and is defined as the concentration at which the neighboring polymer coils start to overlap with each other. It is approximately 0.48 wt % and 0.16 wt % for the 200 and 900 kDa PEO samples, respectively [17,18]. The stock solutions of the two species are prepared by mixing the PEO powder in deionized water that has been filtered using 0.2-μm-pore-size aqueous filters. The solution is kept in an incubator for 10 days at $\sim$40°C to allow the polymer to dissolve completely. The stock solution is shaken very gently to help homogenize the solution. A drop of chloroform is added to prevent bacterial growth in the polymer and sodium chloride is added to ensure consistent salt concentration for all our samples. The salt concentration for all samples reported here is 25 mM.

Polystyrene (PS) spheres with diameters of 0.46 μm, 0.64 μm, 0.65 μm, 0.97 μm, and 2.0 μm are used as probe particles. The 0.65 μm PS beads are sulfate modified while the other sizes of beads are carboxylate-modified latex (CML). All of the beads are significantly larger than the mesh size, which is a few nanometers for the polymer at these concentrations and is calculated using the following equation [18]:

$$\xi=R_g(c^*/c)^{0.75}, \tag{10}$$

where, R_g is the radius of gyration of the polymer, c^* and c denote the overlap concentration for the polymer and the concentration of the sample, respectively, while ξ denotes the mesh size of the semidilute polymer solution. The mo-

lecular weight dependence on the radius of gyration has been experimentally found to be [17]

$$R_g = 0.215 M_w^{0.583 \pm 0.031} \ \text{Å}, \tag{11}$$

where, M_w denotes the molecular weight of the polymer. Since the individual polymer coils are contiguous to each other at c^*, the radius of gyration can be related to the overlap concentration using the following equation [18]

$$c^* = \frac{M_w}{\frac{4}{3} N_A \pi R_g^3}, \tag{12}$$

where N_A is the Avogadro's number.

Previous experiments [19] have shown that there is an adsorbed layer of polymer on the bead surfaces, which depends on the bead size. We use different bead sizes to check whether this adsorbed layer of polymer affects the microrheological measurements.

Diffusing wave spectroscopy experiments are done in the transmission geometry using an Ar^+ laser operating in the TEM_{00} mode with laser emission at $\lambda = 514.5$ nm (*in vacuo*). A convex lens is used to focus the beam to a point on the sample cell. Glass cells (Vitrocom, NJ) with 2.00 mm internal thickness are used for our measurements. Since multiply scattered light is depolarized, the intensity of the scattered light with polarizations both parallel and perpendicular to that of the incident beam will have equal intensities. Since each of these intensities is independent, the signal to noise ratio of the correlation function is reduced, causing the intercept to fall. To circumvent this, a polarization analyzer is placed before the detection system; this restricts the signal to a single polarization, thereby increasing the signal to noise ratio. Scattered light is collected by an optical fiber, and then split by a fiber optic beam splitter and directed to two photomultiplier tubes (PMT's). This *pseudo*-cross-correlation mode is used to help circumvent the dead time of the detector electronics and to reduce after-pulsing effects, making it possible to measure correlations at very short delay times [20]. The signals from the PMTs are directed through a pair of amplifier discriminators, which are connected to a correlator.

The concentrations of the polymer solutions used for our DWS measurements are 2.2, 4, and 6 wt % of the 900 kDa and 6.7, 12.2, and 21.6 wt % of the 200 kDa PEO. These are prepared by diluting more concentrated stock solutions for both molecular weights of the polymer. Polystyrene beads are added so that the bead concentrations in all the samples used in the DWS experiments are at 1 wt %. The samples are thoroughly mixed using a rotator for a period ranging from a few days to about two weeks. This high bead concentration is used to ensure strong multiple scattering for the DWS measurements. The polymer stock and the samples are wrapped in an aluminum foil to avoid photodegradation of the polymer during storage, which ranges from a few days to several weeks. All samples are checked under a microscope for bead aggregation to avoid erroneous DWS results. Intensity correlation functions are collected for 1 h at room temperature. Several of the measurements were repeated to check the reproducibility of the data.

The transport mean free paths l^* of the samples are determined by a separate measurement of the transmitted intensity of light [11]. The transmitted intensity T through a nonabsorbing slab of thickness L is proportional to $(l^*/L)(1 + 4l^*/3L)$ [11], and is obtained by assuming diffusive propagation of light through the sample. This expression for the transmitted light intensity assumes absorbing boundary conditions, with no diffuse flux into the sample from the outside at the boundaries, zero reflectivity at the sample walls, and the absence of any ballistic photons transmitted through the sample. We further assume that the incident flux appears as a diffuse source at a distance l^* inside the sample. Rigorous derivations of the transmitted intensity of the diffused light have been done [21] where the above assumptions have been investigated in detail. In particular, the effects of internal reflections at the sample cell walls, refraction at the interfaces, anisotropic scattering, and the extrapolation length ratio, have all been investigated, and the consequences for the intensity of the transmitted light have been probed experimentally and compared with the theoretical simulations. However, since all our samples are very strongly multiply scattering, the approximate form used in this paper is sufficient, and our experimental error in the estimate of the transport mean free path is approximately 10%. By measuring the ratio of the transmitted intensity of a reference sample whose l^* is known to the transmitted intensity of the PEO/PS sample, we can find the unknown transport mean free path for each PEO/PS sample. As a reference sample, we use solutions of polystyrene beads in water at the same concentration by weight as in the PEO samples. We use the same geometry to measure the transmitted intensity for both the reference and the unknown sample. To determine the value of l^* for the reference sample, we measure the correlation function, acquiring data for 1 h. The functional form of the correlation function for a freely diffusing particle [11] is fit to the data to obtain l^*, the only parameter in the fit, yielding the reference value. The transmitted intensity T for each sample is averaged for 15 min. The time dependent mean square displacements of the beads in the polymer network are then extracted from the correlation functions using these measured transport mean free paths [11].

The single scattering or QELS experiments are performed using a goniometer with a fiber optic detection system and an Ar^+ laser emitting light at 514.5 nm (*in vacuo*) operating in the TEM_{00} mode. Glass tubes with a diameter of 0.5 cm are used as sample cells for these experiments. Quasielastic light scattering measurements are made on 4 wt % 900 kDa PEO sample with three different bead sizes; 0.46 μm, 0.65 μm, and 0.97 μm. The bead concentration that is used for these experiments is ~ 0.0025 wt %; it is adjusted to ensure that scattering from the beads is predominant over that of the polymer itself, while limiting multiple scattering. In order to increase the probability that only singly scattered light is detected, we use a polarizer before the detection optics to block any depolarized light, which arises from remnant multiple scattering. The time averaged intensity correlation func-

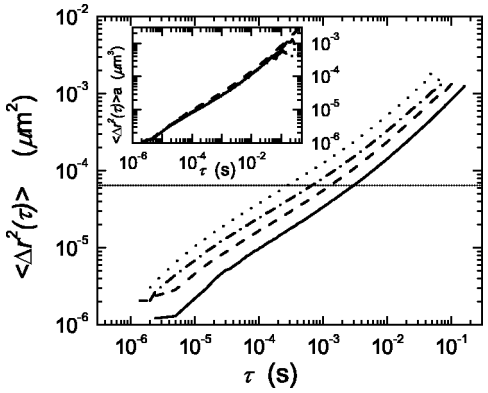

FIG. 2. Plot of the probe dynamics measured by using DWS in a 900 kDa PEO sample solution at a concentration of 2.2 wt % by weight for four different polystyrene (PS) bead sizes. The results for different bead sizes are depicted by the different line styles, 0.46 μm (dotted line), 0.65 μm (dot-dashed line), 0.97 μm (dashed line), and 2.0 μm (solid line). The horizontal dotted line depicts the square of the mesh size for the 2.2 wt % polymer solution calculated using Eq. (10). The scaled mean square displacements are shown in the inset.

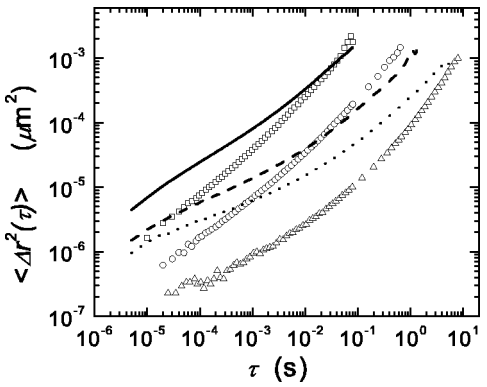

FIG. 3. Mean square displacements for different concentrations of PEO with 0.65 μm PS beads using DWS. The results for the 900 kDa PEO solutions are shown by lines, 2.2 wt % (solid line), 4 wt % (dashed line), and 6 wt % (dotted line) while the 200 kDa PEO solutions are plotted using open symbols, 6.7 wt % (□), 12.2 wt % (○), and 21.6 wt % (△). For the 200 kDa PEO samples every third data point is plotted for clarity.

tions are collected for two to three hours at room temperature. We use Eq. (9) to extract the mean square displacements of the probe particles from the measured correlation functions.

In order to compare the results of microrheology measurements to bulk measurements of viscoelasticity, bulk rheological measurements are performed with a strain-controlled rheometer using double-walled couette geometry for all the polymer concentrations. These measurements are performed in the absence of the probe particles and are done at room temperature. The presence of polystyrene beads has no effect on the bulk rheology measurements and is confirmed by comparing the results for a 4 wt % 900 kDa PEO solution mixed with 1 wt % PS beads with a similar polymer solution without beads. Strain sweeps $[G'(\omega), G''(\omega)$ as functions of the maximum applied strain] of the polymer solutions are carried out to determine the linear region of measurement of the moduli. All subsequent measurements of the frequency dependence of the storage and loss moduli are done at strains sufficiently low to ensure linear response. The measurements are repeated several times to check their reproducibility.

IV. RESULTS

The MSD measured using DWS for different probe sizes suspended in a 2.2 wt %, 900 kDa PEO solution is shown in Fig. 2. Using Eq. (10), we calculate a mesh size of 8 nm for this sample. The horizontal dotted line in the figure depicts the square of the mesh size. The MSD for the different bead sizes show the same trend with τ, with the bigger ones moving over smaller distances than the smaller ones. The plot illustrates the sensitivity of the DWS measurements that can detect bead motions as small as ~ 1 nm, which is a few hundredths of their own size. The smallest displacements we can detect are less than the mesh size while the largest displacements are greater by an order of magnitude. The MSDs for the different probes in Fig. 2 scale very nicely with the bead radius as is shown in the inset. The MSDs for the different probes in Fig. 2 scale with the bead size, which is an initial indication of the independence of the probe size when measuring the moduli of the viscoelastic materials. Figure 3 shows the MSD data for 0.65 μm PS beads in the six different polymer solutions. The data for the 900 kDa PEO solutions are shown by lines while the data for the 200 kDa PEO solutions are shown by symbols. The MSD data for the higher molecular weight polymer concentrations have a smaller logarithmic slope at shorter lag times indicating a more elastic response of the material. At longer lag times, the same species of the polymer show a more viscous like behavior. By contrast, the MSD curves for the lower molecular weight show a more viscous like behavior when compared to the 900 kDa samples. A more elastic response at shorter lag times is evident in the highest concentration of the 200 kDa PEO used in our experiments and is shown in Fig. 3 by open triangles. The monotonic decrease in the MSD with increasing polymer concentration reflects an increase in the complex modulus G^* of the samples, as expected.

Since DWS is able to probe the viscoelastic behavior of our samples at frequencies ranging from $\sim 10^1$ rad/s to $\sim 10^5$ rad/s the data does not always result in a significant overlap with bulk mechanical measurements, which generally lie between 0.01 rad/s and 100 rad/s. Thus, in order to extend the range of our measurements to lower frequencies, the DWS data are complemented by QELS measurements.

The usefulness of QELS can be seen in the results for the 4 wt % 900 kDa PEO sample. This particular polymer concentration is chosen as it exhibits an elastic behavior at shorter lag times. Since the 2.2 wt % polymer concentration is predominantly viscous at the time scales probed by QELS and the 6 wt % polymer solution has a larger polymer background scattering we find this particular concentration to be ideal to test this technique. Figure 4 is a plot of the mean square displacements obtained from single scattering experiments at scattering angles of 20° (△) and 90° (○), and the

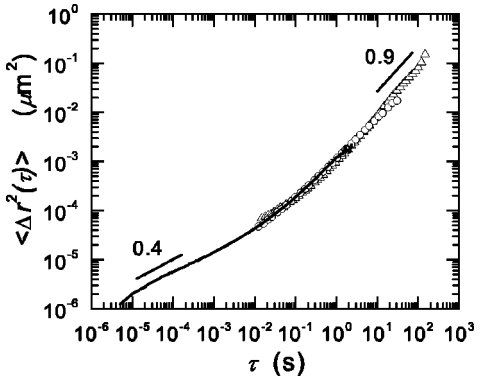

FIG. 4. Mean square displacements obtained from single scattering (open symbols) from a 4 wt % 900 kDa PEO solution with 0.97 μm PS beads and compared with the corresponding DWS measurement (solid line). The QELS data is collected at 20° (△) and 90° (○). Every fourth point is plotted for the QELS data for the purpose of clarity. The DWS measurement probes much shorter time scales than QELS. The initial slope of the data is ~0.4, indicating that the nature of the polymer solution is predominantly elastic while at larger time scales the slope approaches one indicating a more nearly viscous behavior.

corresponding DWS measurement (solid line) for a 4 wt % solution of 900 kDa PEO containing 0.97 μm beads. The plot illustrates the different time scales probed by the two light scattering techniques and shows that the results agree very well except in the small τ limit of the QELS data. The MSD is very sensitive to measurement of $g_1(\tau)$ at short lag times where a small change in the value of the intercept of the correlation function will introduce a significant change in the MSD, leading to considerable experimental uncertainty. The plot also shows that the QELS data taken at different angles overlap with each other, with the data taken at the lower scattering angle extending the measurement by almost a decade. The slope of the MSD data at longer lag times approaches one, indicating a predominantly diffusive behavior of the probe particles, while at early lag times it is approximately equal to 0.4, indicating the presence of a significant elastic component in the response of the polymer. The data taken for 4 wt % 900 kDa PEO samples containing different bead sizes varies in the same manner as seen in the data shown in Fig. 2.

The modified algebraic form of the generalized Stokes-Einstein equations given in Eqs. (5) and (6) is used to calculate the elastic and viscous moduli from the MSD data obtained from the light scattering experiments. The noisy regions of the MSD data are not included in the calculation of the moduli. The MSD data below $\sim 10^{-5}$ s and above ~ 1 s are neglected in DWS measurements. For QELS measurements, only the data in the region $\sim 10^{-1}$ s to ~ 100 s are used for our analysis. This temporal range corresponds to the region where the correlation function decays by 95%. The temporal limits for the data depend on the bead size used as probes, which determines the characteristic decay times of the correlation functions. All of these measurements are compared directly with the bulk rheology measurement. The three plots in Fig. 5 show the comparison between the moduli obtained from microrheology using DWS and QELS

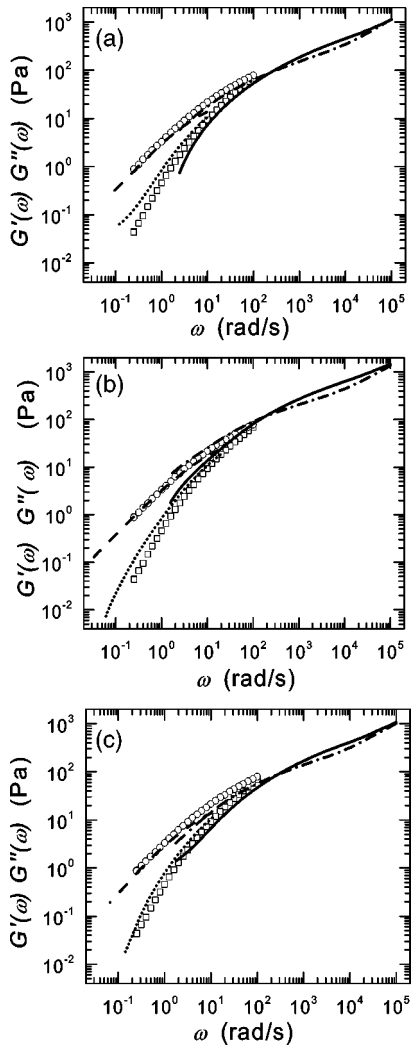

FIG. 5. Storage and loss moduli for 4 wt % 900 kDa PEO obtained from bulk rheology measurements (open symbols) and microrheological measurements (lines). At high frequencies, the elastic and viscous moduli are comparable while the loss or viscous modulus is predominant at lower frequencies. With the help of the two light scattering techniques, DWS (G', solid line; G'', dot-dashed line) and single scattering at 20° (G', dotted line; G'', dashed line), we are able to obtain data over ~6 decades in frequency and a complete overlap with bulk measurements (G', □;G'', ○). The three graphs [(a) 0.46 μm CML, (b) 0.65 μm sulfate, and (c) 0.97 μm CML] depict the different bead sizes that are used as probe particles. The moduli obtained from the light scattering measurements for all the bead sizes show a good agreement with bulk rheology measurements.

to the bulk rheology measurements for the 4 wt % 900 kDa PEO solutions for three different bead sizes. The DWS measurements are shown by the solid and dot-dashed lines for the elastic and viscous moduli, respectively. Measurements of the viscoelasticity of the polymer solution using QELS are shown by the dotted lines for the elastic and dashed lines for the viscous moduli. The bulk rheology measurements are plotted as open symbols using squares for the elastic modulus and circles for the viscous modulus. It is evident from the plots that light scattering and bulk measurements of the vis-

coelastic properties of the polymer solutions are consistent. By combining DWS and QELS results, we obtain the moduli over six decades in frequency with good overlap with the bulk measurements. The moduli obtained from the two scattering techniques coincide very well in the region of frequency in which they overlap. We are able to obtain data at high frequencies where the moduli cross and the elastic modulus dominates, showing the predominantly elastic behavior of the PEO network due to entanglements of the polymer chains. By contrast, at very low frequencies, the response of the network is markedly different and the viscous modulus dominates; this is also evident in the MSD which has a slope that is very close to the one at longer lag times, as shown in Fig. 4. This diffusive behavior of the particle reflects the relaxation of the polymer chains due to reptation, freeing the entanglements.

We have compared the results obtained by using Eqs. (3) and (4) with the results from the modified algebraic forms. The modified equations give an accurate estimate for the moduli when the MSD is highly curved and the slope changes very rapidly as this corresponds to a crossover point in the moduli. Since most of our data are not highly curved the differences in the crossover frequencies between the two algebraic forms are 10–20%. However, for the data shown with open triangles in Fig. 3, the difference in the crossover frequencies is more than 40%.

Local heterogeneities in the polymer solution around the beads may lead to a different value of the moduli that may not reflect the bulk viscoelastic response of the polymer. The heterogeneities might be caused by an adsorbed layer of the polymer on the surface of the probe particles that could depend on the size or surface treatment of the latex beads and on the concentration and molecular weight of the PEO [19]. To investigate the first possibility, we made measurements using three different beads, with varying sizes and different surface treatments. We used 0.46 μm (CML), 0.65 μm (sulfate), and 0.97 μm (CML) diameter beads. As shown in Figs. 5(a), 5(b), and 5(c) the moduli measured by light scattering experiments using the different bead sizes as probes agree with those measured using the rheometer. This suggests that the surface adsorption does not lead to heterogeneities that affect the measurement of the viscoelasticity and that the moduli are not affected by an adsorbed layer on the surface of the beads. As a further check on the possibility of polymer adsorption on the beads, we compare particles of similar size but markedly different surface chemistries. We use 0.65 μm diameter sulfate coated and 0.64 μm diameter CML in a 900 kDa PEO sample at 2.2 wt % and measure the dynamics using DWS. In Fig. 6 we plot the viscoelastic spectra obtained from the MSD data. The solid and the dot-dashed lines denote the elastic and the viscous moduli, respectively, as probed by the sulfate coated beads. The open symbols denote the moduli obtained by using the CML coated beads in a solution of the same polymer concentration. The difference observed between the mean square displacements of the two data sets is $\sim$10% and is within the error of estimating l^*. From the moduli obtained from these two types of beads, we conclude that the two different bead chemistries have no effect on the microrheology results.

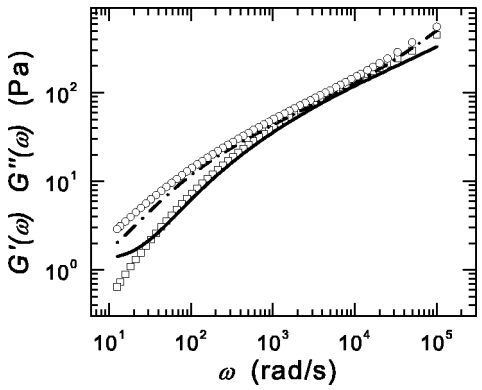

FIG. 6. Effect of different bead surface chemistry. Comparison of storage and loss moduli probed with 0.65 μm sulfate coated (G', solid line; G'', dot-dashed line) and 0.64 μm carboxylate modified (G', □;G'', ○) beads in 2.2 wt % 900 kDa PEO solution measured using DWS. For clarity, every third data point is plotted for the 0.64 μm diameter bead size.

We also investigate the effect on microrheology of any possible polymer adsorption on the surfaces of the beads, as a function of the molecular weight of the polymer. Dynamic light scattering experiments [19,22] on polystyrene beads in dilute solutions of PEO have shown that the polymer chains are adsorbed on the PS beads, resulting in an increase in the hydrodynamic radius of the probes. We use DWS to measure the moduli of solutions of 200 kDa PEO at three different concentrations, 6.7 wt %, 12.2 wt %, and 21.6 wt %. The three plots in Fig. 7 show microrheology and bulk rheology measurements for the 200 kDa PEO polymer sample at these concentrations. The measurements shown in the figure are done with polystyrene beads with a diameter of 2.0 μm (CML) for the 6.7 wt % solution and 0.65 μm (sulfate) for the other two polymer concentrations. The open symbols are the bulk measurements and the solid and dot-dashed lines represent the data obtained from the DWS measurements. The three graphs clearly show the excellent similarity between the elastic and the viscous moduli obtained from the two different types of measurement. The DWS measurements are able to extend the frequency range of the viscoelastic spectrum by almost three decades. The graphs in Fig. 5 and 7 together show that light scattering microrheology measurements are not affected by any adsorbed layer of polymer on the beads for the different combinations of bead sizes, polymer sizes and polymer concentrations investigated here.

Using different concentrations and molecular weights of the polymer also enables us to investigate different viscoelastic properties. The lowest concentration of the 200 kDa polymer used here is predominantly viscous over the entire range of our measurements. The higher frequency DWS measurements only suggest a crossover at even higher frequencies not probed by our measurements. On increasing the concentration of this polymer, the DWS measurements show the crossover of the two moduli. By contrast, the 900 kDa polymer solutions show a distinct crossover at all the three concentrations investigated. The crossover frequency is shifted to lower frequencies for the higher molecular weight poly-

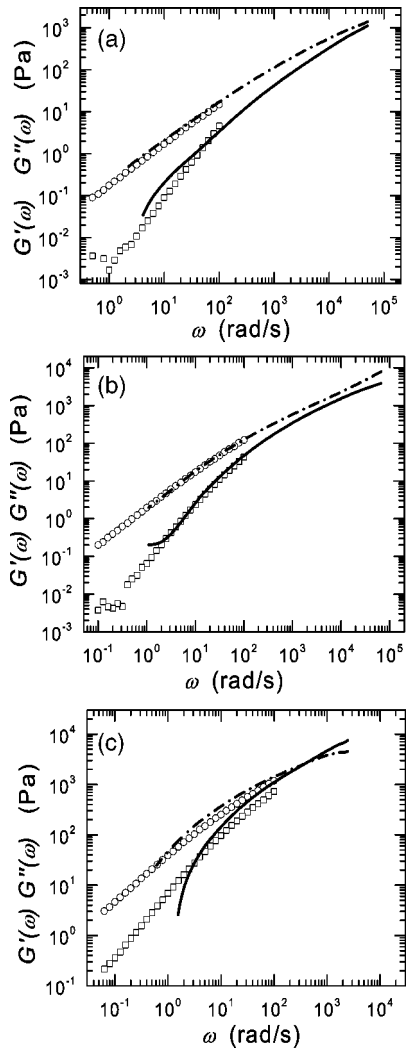

FIG. 7. Storage and loss moduli for 200 kDa PEO obtained from DWS (G', solid line; G'', dash-dotted line) and bulk measurements (G', □;G'', ○) for three concentrations of the polymer, (a) 6.7 wt % with 2.0 μm (b) 12.2 wt % with 0.65 μm, and (c) 21.6 wt % with 0.65 μm PS beads. The comparisons between the two types of measurements show a very good agreement in each case.

mer. This shift of the relaxation time between the two molecular weights of the polymer is consistent with the reptation models of polymer dynamics. Owing to its larger chain length, the bigger polymer will take a longer time to reptate through the network, and this will result in a crossover at a lower frequency when compared to a polymer with a shorter chain length. In all cases, the light scattering microrheology data compares very well with the bulk measurements over the full region of overlap.

Finally, we compare a PEO solution that was prepared 20 days prior to the experiment to a set of PEO samples that had been prepared more than three months earlier. The samples were 900 kDa PEO at a concentration of 4% by weight. The measurements were all performed with DWS. The correlation functions for the old PEO samples decay a bit more slowly than the new samples but on extracting the frequency dependant moduli and comparing them with previous measurements, we observe no significant aging effects of the polymer that result in changed moduli. We conclude that the aging of the polymer solution is not a significant factor in our measurements.

V. CONCLUSIONS

We show that two different dynamic light scattering techniques can be used to measure the viscoelastic properties of a simple flexible polymer that is not permanently cross linked. Employing both DWS and conventional single scattering DLS, we extend the range of the viscoelastic data over seven decades. We use an algebraic form of the generalized Stokes-Einstein relation and avoid numerical transformations of our data or using functional forms to fit the modulus in Laplace frequency space. As such, no prior knowledge or model for the viscoelastic behavior is required to interpret and analyze the light scattering data. The viscoelastic spectra of the polymer obtained from the light scattering measurements agree with bulk measurements at all polymer concentrations. Our results show that the viscoelastic response of the probe particles is independent of its size or surface chemistry. These experiments demonstrate convincingly that microrheology works very well when applied to uncross-linked polymer suspensions, using probe particles as the scatterers. Further experiments are required to test the validity of microrheology for systems that are more complex, where sample heterogeneities might limit its validity; in particular, the important case of cross-linked polymer suspensions must be investigated.

ACKNOWLEDGMENTS

The authors would like to thank V. Trappe, P.N. Segre, and M.T. Valentine for useful discussions. This work was supported by NSF (Grant Nos. DMR-9971432 and DMR-9704300).

[1] J.D. Ferry, *Viscoelastic Properties of Polymers* (Wiley, New York, 1980).

[2] P. M. Chaikin and T. Lubensky, *Principles of Condensed Matter Physics* (Cambridge University Press, Cambridge, 1995).

[3] F.C. MacKintosh and C.F. Schmidt, Curr. Opin. Colloid Interface Sci. **4**, 300 (1999); T. Gisler and D.A. Weitz, *ibid.* **3**, 586 (1998).

[4] T.G. Mason and D.A. Weitz, Phys. Rev. Lett. **74**, 1250 (1995).

[5] T. Gisler and D.A. Weitz, Phys. Rev. Lett. **82**, 1606 (1999).

[6] A. Palmer, T.G. Mason, J. Xu, S.C. Kuo, and D. Wirtz, Biophys. J. **76**, 1063 (1999).

[7] F. Gittes, B. Schnurr, P.D. Olmsted, F.C. MacKintosh, and C.F. Schmidt, Phys. Rev. Lett. **79**, 3286 (1997); B. Schnurr, F. Gittes, F.C. MacKintosh, and C.F. Schmidt, Macromolecules **30**, 7781 (1997).

[8] T.G. Mason, K. Ganesan, J.H. van Zanten, D. Wirtz, and S.C.

Kuo, Phys. Rev. Lett. **79**, 3282 (1997).
[9] B.J. Berne and R. Pecora, *Dynamic Light Scattering: With Applications to Chemistry, Biology and Physics* (Wiley, New York, 1976).
[10] D.J. Pine, D.A. Weitz, P.M. Chaikin, and E. Herbolzheimer, Phys. Rev. Lett. **60**, 1134 (1988).
[11] D.A. Weitz and D.J. Pine, *Dynamic Light Scattering*, edited by W. Brown (Oxford University Press, Oxford, 1992).
[12] G. Maret and P.E. Wolf, Z. Phys. B: Condens. Matter **65**, 409 (1987).
[13] A.V. Tobolsky, J. Appl. Phys. **27**, 673 (1956).
[14] T.G. Mason, Rheol. Acta **39**, 371 (2000).
[15] T.G. Mason, Hu Gang, and D.A. Weitz, J. Mol. Struct. **383**, 81 (1996).
[16] J.C. Crocker, M.T. Valentine, E.R. Weeks, T. Gisler, P.D. Kaplan, A.G. Yodh, and D.A. Weitz, Phys. Rev. Lett. **85**, 888 (2000).
[17] K. Devanand and J.C. Selser, Macromolecules **24**, 5943 (1991).
[18] E.C. Cooper, P. Johnson, and A.M. Donald, Polymer **32**, 2815 (1991).
[19] E. Killmann and P. Sapuntzjis, Colloids Surf., A **86**, 229 (1994).
[20] H.C. Burstyn and J.V. Sengers, Phys. Rev. A **27**, 1071 (1983).
[21] D.J. Durian, Phys. Rev. E **50**, 857 (1994); **51**, 3350 (1995); M.U. Vera and D.J. Durian, *ibid.* **53**, 3215 (1996); J.X. Zhu, D.J. Pine, and D.A. Weitz, Phys. Rev. A **44**, 3948 (1991); P.-A. Lemieux, M.U. Vera, and D.J. Durian, Phys. Rev. E **57**, 4498 (1998).
[22] M.A.C. Stuart, F.H.W.H. Waajen, T. Cosgrove, B. Vincent, and T.L. Crowley, Macromolecules **17**, 1825 (1984).